Universidade de Aveiro
2021

FILIPA FERREIRA LEANDRO

EFFECTS OF THERMAL STRESS ON THE PHOTOINACTIVATION AND REPAIR OF PHOTOSYSTEM II IN A XANTHOPHYLL CYCLE-DEFICIENT GREEN ALGA

EFEITOS DO STRESS TÉRMICO NA FOTOINATIVAÇÃO E REPARAÇÃO DO FOTOSSISTEMA II NUMA ALGA DEFICIENTE DO CICLO DAS XANTOFILAS

Universidade de Aveiro
2021

FILIPA FERREIRA LEANDRO

EFFECTS OF THERMAL STRESS ON THE PHOTOINACTIVATION AND REPAIR OF PHOTOSYSTEM II IN A XANTHOPHYLL CYCLE-DEFICIENT GREEN ALGA

EFEITOS DO STRESS TÉRMICO NA FOTOINATIVAÇÃO E REPARAÇÃO DO FOTOSSISTEMA II NUMA ALGA DEFICIENTE DO CICLO DAS XANTOFILAS

Dissertação apresentada à Universidade de Aveiro para cumprimento dos requisitos necessários à obtenção do grau de Mestre em Biologia Aplicada, realizada sob a orientação científica do Professor Doutor João António de Almeida Serôdio, Professor Auxiliar com Agregação do Departamento de Biologia da Universidade de Aveiro, e Doutora Ana Cristina de Fraga Esteves, Investigadora Auxiliar do Departamento de Biologia da Universidade de Aveiro.

You're gonna rattle the stars, you are!
~ Treasure Planet

o júri

Presidente	Dra. Isabel Maria Cunha Antunes Lopes Investigadora Principal em Regime Laboral do Departamento de Biologia da Universidade de Aveiro
Arguente	Dr. Gregor Christa Research Assistant at University of Wuppertal
Orientador	Prof. Dr. João António de Almeida Serôdio Professor Auxiliar com Agregação do Departamento de Biologia da Universidade de Aveiro

agradecimentos

Com o fim desta etapa, olho para o meu percurso académico com nostalgia e apreciação. Quero agradecer a todos os que me acompanharam e o tornaram possível.

Ao meu orientador, Professor Doutor João Serôdio, pela confiança, disponibilidade, compreensão, auxílio e orientação. Um enorme obrigado professor!

À minha coorientadora, Doutora Ana Cristina Esteves, pela paciência infinita, as palavras de incentivo, compreensão e orientação. Muito obrigada, Cristina!

Ao meu companheiro, Leandro, simplesmente por me aturar em todos os momentos. Obrigada por me incentivares e acreditares em mim sem duvidar!

À minha filha, que mostrou o que é resiliência. Amo-te mais que tudo!

A toda a minha família, que me incentivou a continuar, sempre me apoiou e foi a base que permitiu que pudesse prosseguir os meus estudos.

Aos meus amigos do laboratório, Luísa, Cláudio e Cátia por todos os bons momentos que passamos, tornaram esta 'estadia' mil vezes mais divertida. Agradeço à Silja também pela disponibilidade e ajuda que me deu.

Às minhas amigas por me ouvirem falar de algas e proteínas, mesmo não gostando.

Sinto uma enorme gratidão por todos vós, fizeram desta experiência ainda melhor.

palavras-chave

Fluorescência de clorofila, Proteína D1, Fotoinibição, Fotossistema II, Reparação, Temperatura

resumo

A fotossíntese e a produtividade primária dependem profundamente da temperatura. Temperaturas extremamente altas ou baixas afetam os mecanismos enzimáticos de fotoproteção (ciclo das xantofilas) e exacerbam os danos provocados pela irradiação elevada no fotossistema II (PSII). Uma hipótese recentemente proposta afirma que o stress abiótico, incluindo frio e calor moderado, aumenta a fotoinibição da fotossíntese não por efeitos diretos no PSII, mas sim pela inibição dos mecanismos de reparação. Este trabalho pretende testar essa hipótese num grupo ainda inexplorado de algas verdes (Bryopsidales) que não possuem um ciclo das xantofilas funcional.

Para testar esta hipótese, recorremos a medições da fluorescência da clorofila a, sob stress luminoso e térmico, e posterior quantificação da proteína D1, através da técnica do Western blot. Os nossos resultados mostraram que, para este grupo de algas, a hipótese acima mencionada, não é aplicável, pois os stresses abióticos afetaram não apenas os mecanismos de reparo, mas também exacerbaram a fotoinibição. Consequentemente, o grupo de algas verdes (Bryopsidales) apresentou um grande potencial para futuros estudos no âmbito da investigação dos mecanismos de reparação do fotossistema II.

keywords

Chlorophyll Fluorescence, D1 protein, Photoinhibition, Phototosystem II, Repair, Temperature

abstract

Photosynthesis and primary productivity are very temperature-dependent. Extremely high or low temperatures affect the enzymatic mechanisms of photoprotection (xanthophyll cycle) and exacerbate the photo-imaging effects of high light on photosystem II (PSII). A recently proposed hypothesis states that abiotic stress, including mild cold and heat, enhances photoinhibition of photosynthesis not by directly damaging the PSII, but by inhibiting repair mechanisms. This work intends to test this hypothesis in an as yet unexplored group of green algae (Bryopsidales) without a xanthophyll functional cycle.
In order to test this hypothesis, we used the measurement of chlorophyll fluorescence, under light and thermal stress, and subsequent quantification of D1 protein, using the Western blot technique. Our findings showed that for this group of algae, the aforementioned hypothesis is not applicable, as the abiotic stresses affected not only repair mechanisms but also exacerbated photoinhibition. Consequently, the group of green algae (Bryopsidales) showed great potential for future studies in the scope of the investigation regarding repair mechanisms of photosystem II.

Index

LIST OF FIGURES 2

LIST OF TABLES 4

1. INTRODUCTION 5

2. MATERIALS AND METHODS 10

2.1 SAMPLE ORIGIN AND GROWTH CONDITIONS 10

2.2 CHLOROPHYLL FLUORESCENCE MEASUREMENTS 10

2.3 LIGHT STRESS-RECOVERY EXPERIMENTS 10

2.3.1 Experimental setup *10*

2.3.2 PSII photoinactivation and repair rates *11*

2.4 PHOTOACCLIMATION STATE 14

2.5 PROTEIN EXTRACTION 16

2.6 PROTEIN QUANTIFICATION 16

2.7 WESTERN BLOT 17

2.7.1 Sample preparation *17*

2.7.2 Gel electrophoresis *18*

2.7.3 Transfer *20*

2.7.4 Protein detection *20*

3. RESULTS 24

3.1. VARIATION OF K_{PI} AND K_{REC} WITH TEMPERATURE 24

3.2. HYSTERESIS LIGHT-RESPONSE CURVES 28

3.3. D1 PROTEIN QUANTIFICATION AND RESPONSE TO TEMPERATURE 29

4. DISCUSSION 32

4.1. EFFECTS OF TEMPERATURE ON PSII PHOTOINACTIVATION AND REPAIR 32

4.2. EFFECTS OF THERMAL STRESS ON LIGHT-INDUCED LOSS OF D1 CONTENT 33

4.3. THE 'NEW PARADIGM' IN XC-DEFICIENT BRYOPSIDALES 34

5. REFERENCES 36

List of Figures

Figure 1 l Schematic representation of D1 protein repair cycle. Adapted from Ohnishi & Murata (2006). FtsH and DegP2 are a type of protease reported as responsible for D1 protein proteolysis.....7

Figure 2 l Schematics of the 3D-printed cuvette holder and water jacket, showing the internal positioning of the cuvettes **(A)** and the assemblage with the LED panel with 4 LEDs for each cuvette **(B)**.....11

Figure 3 l A – Experimental setup: Multi-Color PAM **(1)**, measuring unit **(2)**, water jacket **(3)**, LED panel **(4)** and water bath **(5)**; **B** – Measuring unit **(2)** with glass cuvette; **C** – Empty water jacket **(3)**; **D** – Samples in the water jacket **(3)** with LED panel **(4)** on.....12

Figure 4 l Schematics of the experiment workflow for posterior quantitative analysis of the D1 protein by western blot. Two different time points were used t_0 and t_f. All samples were incubated in dark for two hours in the presence or absence of the protein inhibitor. After incubation period, samples were exposed at different temperatures, 10, 20 or 35 °C, for 15 minutes in dark, and were immediately flash freeze (t_0 and t_{0L}). The t_f and t_{fL} samples, were further exposed to a high light treatment for two hours, followed by 15 minutes in dark for recovery and immediately flash freeze. See Table 1 for notation.....13

Figure 5 l Gel cassette preparation. Assembly steps follow crescent number order. Adapted from Bio-Rad Mini-PROTEAN® 3 Cell Assembly Guide.....18

Figure 6 l Sandwich assembly for wet transfer **(A)** and preparation for protein transfer using the Mini-Trans-blot apparatus **(B).** Adapted from Kurien & Scofield, 2019.....20

Figure 7 l Variation of F_v/F_m over time, between pre-light stress and recovery in dark at 5 temperatures, in the absence or presence of lincomycin (light-blue circles or dark-blue squares, respectively). F_v/F_m values were measured at 5°C **(A)**, 10°C **(B)**, 20°C **(C)**, 25°C **(D)** and 35°C **(E)**. All measurements were performed in biological triplicates and error bars indicate one standard deviation.....25

Figure 8 l Variation of F_v/F_m (pre-stress) and $\%F_v/F_m$ with temperature. All measurements were performed in biological triplicates and error bars represents one standard deviation.....26
Figure 9 l Variation of the rate constants of photoinactivation, k_{PI}, with temperature, and variation of recovery of inactivated PSII, k_{REC}, opposed to k_{PI}. All measurements were performed in biological triplicates and error bars represents one standard deviation.....27
Figure 10 l Variation of energy-dependent non-photochemical quenching index, qE, with temperature. All measurements were performed in biological triplicates and error bars represent one standard deviation.....27
Figure 11 l Hysteresis light-response curves of *PSII* relative electron transport rate, rETR **(A)** and non-photochemical quenching index yield Y(NPQ) **(B)**. Ascending curves in light blue and descending curves in dark blue. All measurements were performed in biological triplicates and error bars represent one standard deviation.....28
Figure 12 l D1 protein of Photosystem II standard curve obtained by quantification of the D1 immunoblot signal (Adjusted total band volume in arbitrary units). PsbAlD1 protein of PSII positive control/quantitation standard (Agrisera).....29
Figure 13 l Samples D1 concentration in the beginning and at the end of the experiment (t_0, t_{0L} and t_f, t_{fL}, respectively) in the presence or absence of lincomycin (columns with and without pattern, respectively) at the different temperatures.....30
Figure 14 l D1 concentration ratio (t_{fL} /t_{0L}) after highlight treatment obtained by quantification of the D1 immunoblot signal, normalized by the total protein content, in the presence of lincomycin, compared to the percentage of F_v/F_m recovery under the different temperatures……31

List of Tables

Table 1 – Notation. 15
Table 2 – Protein extraction buffers. 16
Table 3 – Laemmli SDS sample buffer. 17
Table 4 – SDS-PAGE Gels. 19
Table 5 – SDS-PAGE running buffer. 19
Table 6 – Towbin buffer with SDS. 21
Table 7 – Tris buffered saline. 21
Table 8– Blocking buffer. 22
Table 9– Staining and destaning solutions. 22
Table 10 – Antibody solutions. 22
Table 11 – Enhanced chemiluminescence (ECL) reagents 23
Table 12 – rETR light-response curve parameters (α, $rETR_m$ and E_k) for the light-increasing and light-decreasing parts of the LC. 29
Table 13 – Y(NPQ) light-response curve parameters ($Y(NPQ_m)$, E_{50} and n) for the light- increasing part of the LC. 29

1. Introduction

The Chlorophyta is a large and diverse group of algae, commonly known as 'green algae', due to their characteristic green coloration, essentially due to the presence of chlorophyll (Chl) *a* and *b* in the same proportion as in higher plants (Bold & Wynne, 1985). Chl *a* is the most abundant chlorophyll, being found in the photosystems of cyanobacteria, algae, and higher plants (Larkum, 2003).

The Ulvophyceae are a group of the Chlorophyta that can have unicellular, colonial, or multicellular forms (Handrich et al., 2017). The Bryopsidales is an order of the class Ulvophyceae that comprises more than 600 species (www.algaebase.org) and that is best known for its morphological diversity, presenting morphologies ranging from uni- to multicellular forms (Handrich et al., 2017). The Bryopsidales are both multicellular and coenocytic (also referred to as siphonous algae) because they are composed of multiple cells, each of which contains multiple nuclei (Umen, 2014) so that the entire thallus can be considered as a single multinucleate cell (Giovagnetti et al., 2018). Being predominantly marine, Bryopsidales occur essentially in subtropical and warm tropical waters with regular salinity levels. Usually, with simple observation, they can be easily spotted in shallow waters, sea-grass beds, or attached to corals notwithstanding that some can survive in considerable deeper waters, also they can be potentially invasive (Lam & Zechman, 2006; Verbruggen et al., 2009).

Photosynthesis is a process of enormous biological importance through which autotrophic life forms harvest light to produce organic matter and oxygen to be used by the metabolism of the heterotrophs. Oxygenic photosynthesis is sunlight dependent. The energy absorbed is used in the conversion of carbon dioxide and water into carbohydrates and oxygen, through the electron transfer between photosystems II and I (PSII and PSI) (Christa et al., 2017; Giovagnetti et al., 2018).

Photosynthesis is also fascinatingly effective since it captures almost all the energy of the light it absorbs (Herrmann & Westhoff, 2001). However, photosynthesis has a major downside, paradoxically caused by light. Due to the production of oxygen reactive species by the photosynthetic process, the electron-transport activity of photosystem II (PSII) and oxygen evolution may suffer significant losses induced by light, through a process globally described as photoinhibition of photosynthesis (Tyystjärvi, 2013). Photoinhibition is defined as a persistent decrease in the efficiency of energy conversion associated with a

decrease of the capacity for photosynthesis associate to the production of reactive oxygen species (ROS) (Demmig-Adams & Adams, 2016). Reactive species of oxygen such as hydrogen peroxide (H_2O_2) and singlet oxygen ($^1O_2$) are by-products of photosynthesis resulting from the photosynthetic electron transport and energy excitation (Nishiyama & Murata, 2014). The production of ROS increases when cells are exposed to strong light, and photoinhibition was shown to be enhanced when intracellular concentrations of ROS increase (Nishiyama et al., 2001).

The persistent or slowly recovering nature of this process, and its dependency on chloroplast synthesis (Greer et al., 1986; Kok, 1956; Tyystjärvi & Aro, 1996), distinguishes it from the reversible downregulation of PSII by nonphotochemical quenching (NPQ) often named as 'dynamic photoinhibition' (Tyystjärvi, 2013). NPQ is a crucial physiological mechanism, thought to have an important photoprotective role by reducing the production of ROS (Handrich et al., 2017). NPQ is the fastest response to excess light, and involves the quenching of singlet excited state chlorophylls via enhanced internal conversion to the ground state, thus harmlessly dissipating excess excitation energy as heat (Christa et al., 2017).

NPQ occurs in almost all algae and higher plants, helping to regulate and protect photosynthesis in environments where light energy absorption exceeds the capacity for light utilization. In green algae, NPQ involves conformational changes within the light harvesting proteins of PSII that, under exposure to high light, cause the reversible conversion of violaxanthin (Vx) into the intermediate xanthophyll antheraxanthin (Ax) and then finally to zeaxanthin (Zx), a process known as the xanthophyll cycle (XC) (Goss & Latowski, 2020). Through the de-epoxidation of Vio into Zea, excess excitation energy is dissipated from the PSII, thus reducing ROS accumulation and light-induced inactivation and damage to the photosystem apparatus (Demmig-Adams & Adams, 1996; Goss & Jakob, 2010).

Other photoprotective mechanisms, such as enzymatic and non-enzymatic systems, get into action against ROS as well. When cells are exposed to stressful conditions, ROS scavenging enzymes, like the superoxide dismutase, catalase and peroxidase as well as antioxidants like ascorbate, glutathione, phenolic compounds and tocopherols, act to control the level of ROS (Blokhina et al., 2003).

When these photoprotective mechanisms are not fully efficient in eliminating ROS, its accumulation induces damage to a core component of PSII reaction center (Handrich et al., 2017), the D1 protein.

The D1 protein is the primary damage target of photoinhibition (Rantala et al., 2021), and conjointly with D2 subunit, binds the pigment cofactors, such as chlorophyll (Komenda, 2000)(Armbruster et al., 2010). The photoinactivation of the D1 protein is continuously counteracted by repair processes (Fig. 1). This repair process, causing D1 turnover, involves the proteolytic degradation of D1, the total removal of degraded protein followed by synthesis of the D1 precursor, processing of the precursor, and finally insertion of freshly *de novo* synthesized D1 into the PSII to re-establish photochemical activity (Aro et al., 1993a). When the photodamage rate surpasses the capacity of the repair process, inactivated PSII complexes start to accumulate (Aro et al., 1993b). Photoinactivation of PSII can be observed and measured when the rate of *de novo* synthesis of D1 protein is inhibited. Lincomycin, a chloroplast synthesis inhibitor that inhibits the early steps in peptide bond formation before polysome assembling (Klaff & Gruissem, 1991), is commonly used to inhibit D1 protein synthesis, aggravating net photoinhibition without causing significant side effects (Aro et al., 1993; Tyystjärvi et al., 1992).

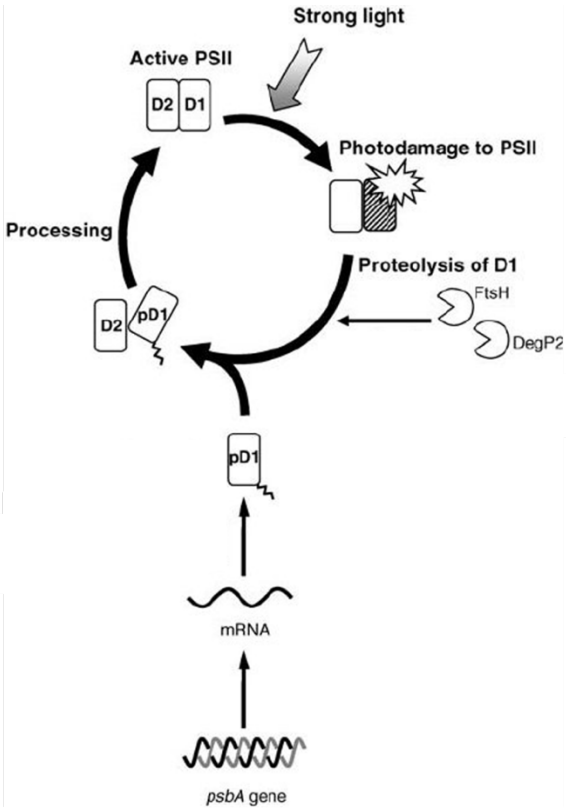

Figure 1 | Schematic representation of D1 protein repair cycle. Adapted from Ohnishi & Murata (2006). FtsH and DegP2 are a type of protease reported as responsible for D1 protein proteolysis.

The repair of D1 protein is negatively stilted by environmental stress factors such as high irradiance, high and low temperatures, salinity, limited nutrients, water availability and others (Demmig-Adams & Adams, 2016; Rantala et al., 2021). Photoinhibitory temperature effects on plants and algae are well known. One of the most thermosensitive sites is PSII (Henley et al., 2002). Limitation of electron transport and carbon fixation by low temperatures, minimize the ability of the plant to use light, and as an outcome, the excess light energy provokes photoinhibition by damaged PSII apparatus (Davison, 1991). Photosynthesis inhibition through heat stress is related to a rupture of energy transfer between phycobilisomes and PSII (Kuebler et al., 1991). Photorespiration can also be affected by light-saturated photosynthesis under high temperatures (Davison, 1991).

The relative importance of photoprotection mechanisms in precenting PSII photoinactivation and PSII repair processes has been the object of intense debate in recent years. An hypothesis (the 'new paradigm' of photoinhibition) has been put forward stating that abiotic stress, including cold and moderate heat, enhances the photoinhibition of photosynthesis not through direct damage to PSII, but through the inhibition of repair mechanisms (Nishiyama & Murata, 2014). This hypothesis has been validated mainly on cyanobacteria but has been studied only marginally in other algal groups.

The major goal of this study is to test this hypothesis, evaluating it in a previously unexplored group of green algae (Bryopsidales), that has the particularity of lacking the main photoprotection mechanism, the xanthophyll cycle. In fact, recent studies on the Bryopsidales showed that the short-term inducible NPQ is not related either with pH-dependent mechanisms nor with the XC activity. In addition to the lack of a functional XC, the *qE* component of NPQ is also absent (Christa et al., 2017). This fact rouse our curiosity towards this unexplored group of algae, its distinctive photophysiology and concomitant responsiveness to abiotic stressors.

In this study, we investigated the temperature effects in the marine green alga *Bryopsis hypnoides* Lamouroux, a species representative of the XC-deficient Bryopsidales. Possessing a dark green color, they are generally described as filamentary tufts, with irregular branching patterns. The majority of studies concerning this species are focused on their extraordinary ability to rapidly aggregate their cell contents when these are extruded into seawater, posteriorly forming protoplasts, regenerating a cell wall within hours and prosper into a functional algal thalli (Li et al., 2009; Lü et al., 2011a; Wang & Tseng, 2006; Ye et al., 2005).

Our study can be considered as pioneer regarding this species, as it was centered on the comparison of the effects of thermal stress on PSII photoinactivation and repair rates through measurements of *in vivo* chlorophyll fluorescence indices and quantification of D1 protein.

2. Materials and Methods

2.1 Sample origin and growth conditions

Specimens of *Bryopsis hypnoides* strain nr.7.86 were purchased from the Experimental Phycology and Culture Collection of Algae at the University of Göttingen, Germany (EPSAG). The algae were cultured at 18 °C under 12 h day / 12 h night cycle at 25 µmol photons $m^{-2}s^{-1}$ provided by white fluorescence lamps (Philips, TL-D 36W/54), in Guillard's F/2 medium (Guillard & Ryther, 1962), with constant aeration to insure continuous movement of the thalli. Fresh medium was supplied every week to keep the algae in an optimum state.

2.2 Chlorophyll fluorescence measurements

In vivo chlorophyll fluorescence was measured using a pulse amplitude modulated fluorometer (Multi-Color PAM, using the ED-101US/MD optical unit, controlled by the PamWin V3.12w software; Heinz Walz, Effeltrich, Germany). Samples were measured in 1.25 mL fresh F/2 medium, supplemented with 4 mM $NaHCO_3$. A blue LED (440 nm) was used for the measuring light, and a white LED (420-645 nm) was used for providing actinic light and for the saturating light pulses (> 4000 µmol photons m^{-2} s^{-1}). In the MCP-D detector unit of the fluorometer, an RG 665 long pass filter (> 650 nm, 3 mm RG665, Schott) was used.

2.3 Light stress-recovery experiments

2.3.1 Experimental setup

A newly developed experimental system was used that allowed to simultaneously expose multiple samples to high light conditions under controlled temperature. This platform consists of a temperature-controlled cuvette holder, formed by a 3D-printed 'water jacket' (Fig. 2A) connected to a water bath (P Select, Frigiterm, Spain). The cuvette holder has openings at the bottom, allowing to illuminate up to six samples (in 1-cm path cuvettes) from below. The cuvette holder was positioned on top of a RGBW LED panel (Serôdio et al., 2018) (Fig. 2B).

By illuminating each sample with four LEDs, the system allowed to deliver white light of 1440 µmol photons m^{-2} s^{-1}.

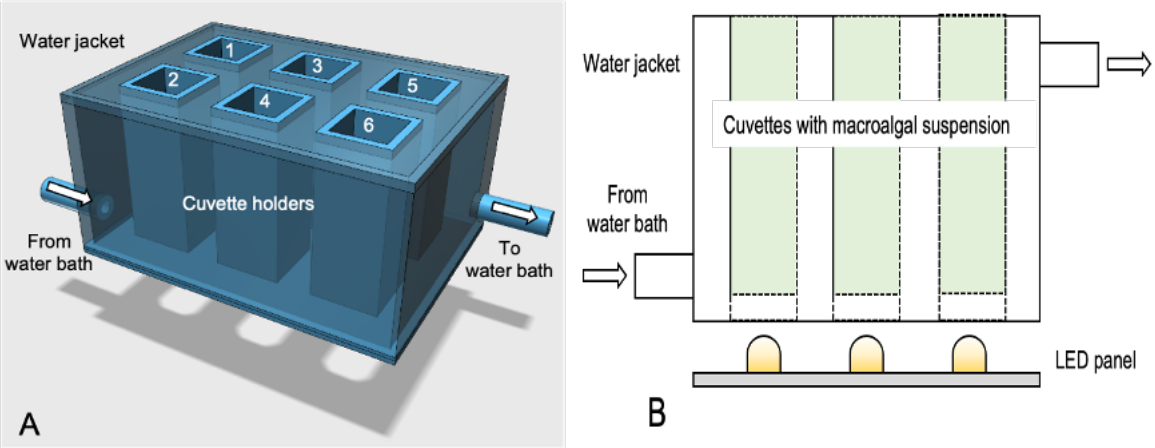

Figure 2 | Schematics of the 3D-printed cuvette holder and water jacket, showing the internal positioning of the cuvettes **(A)** and the assemblage with the LED panel with 4 LEDs for each cuvette **(B)**.

Preliminary tests were performed using seawater to confirm the capacity of this setup to reach and maintain the desired temperatures. Additionally, to ensure light intensity was the same and equally distributed in all cuvettes, a Walz spherical microsensor was placed at middle of the sample height. The system (Fig. 3) was used to expose the samples to 5, 10, 20 (growth temperature), 25 and 35 °C. In each experiment, fresh-cut thalli of *Bryopsis hypnoides* of ca. 1.2 mg (fresh weight) were used in each cuvette.

2.3.2 PSII photoinactivation and repair rates

PSII photoinactivation and repair was quantified by exposing samples to supersaturating light either in the absence or the presence of lincomycin, an inhibitor of prokaryotic gene translation, following Campbell & Tyystjärvi (2012). Photoinactivation of PSII can be observed and measured when the rate of *de novo* synthesis of D1 protein is inhibited. Lincomycin was used to inhibit D1 protein synthesis, aggravating net photoinhibition without causing other side effects (Aro et al., 1993). Three untreated and three lincomycin-treated replicated samples were incubated for 2 h in the dark at growth temperature (same as indicated above)

before the start of the experiment. This period of time was confirmed beforehand to be sufficient to allow the lincomycin solution to penetrate the algae tissue and act effectively (Christa et al., 2018). Lincomycin hydrochloride monohydrate (Alfa Aaser, USA) was added at a concentration of 20 mM lincomycin (pH adjusted to 8.1, the same as the solution of F/2 with $NaHCO_3$), prepared from a fresh stock solution. The salinity of the solutions was verified and adjusted if necessary. After this period, the maximum quantum yield of PSII (F_v/F_m, where $F_v = F_m - F_o$ and F_m and F_o are the maximum and minimum fluorescence emitted by dark adapted samples, respectively) was measured at 5 min intervals for 15 min to determine the pre-stress reference state. The samples were then exposed to supersaturating irradiance of 1440 µmol photons m^{-2} s^{-1} white light for 2 h, to induce photoinhibitory stress in PSII. The LED panel was then turned off and F_v/F_m was measured every 5 minutes for 15 minutes (Fig. 4). After each experiment, samples were flash frozen in liquid nitrogen and stored at -80 °C for protein analysis (see below).

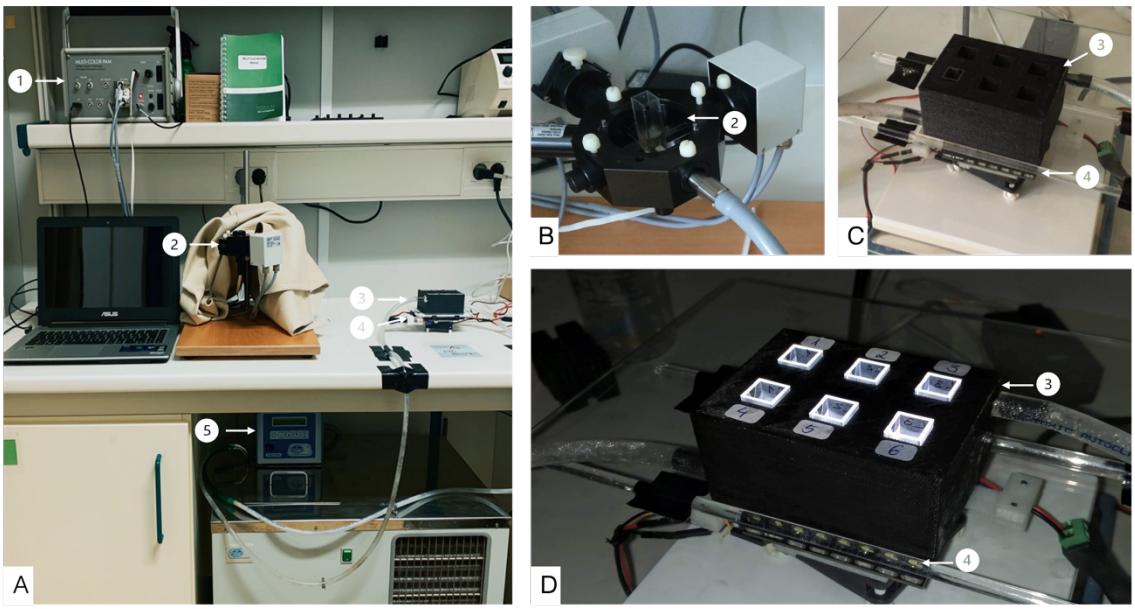

Figure 3 | A - Experimental setup: Multi-Color PAM **(1)**, measuring unit **(2)**, water jacket **(3)**, LED panel **(4)** and water bath **(5)**; **B** - Measuring unit **(2)** with glass cuvette; **C** - Empty water jacket **(3)**; **D** - Samples in the water jacket **(3)** with LED panel **(4)** on.

The rate constant of PSII inactivation, k_{PI} (s^{-1}), was calculated from the decrease in F_v/F_m (expressed as percentage of pre-illumination levels, $\%F_v/F_m$) in

lincomycin-treated samples, considering the time of exposure (T = 120 min) of the applied irradiance (E = 1440 µmol photons m^{-2} s^{-1}) (Campbell & Tyystjärvi, 2012), by

$$k_{PI} = \frac{\ln\left(\%F_v/F_m\right)}{T} \quad (1)$$

Using the value of k_{PI} thus calculated, the rate constant of PSII repair, k_{REC}, was estimated from (Campbell & Tyystjärvi, 2012):

$$\%F_v/F_m = \frac{k_{REC}+k_{PI}e^{-(k_{PI}+k_{REC})T}}{k_{PI}+k_{REC}} \quad (2)$$

Eq. (2) was solved numerically for k_{REC} using MS Excel Solver.

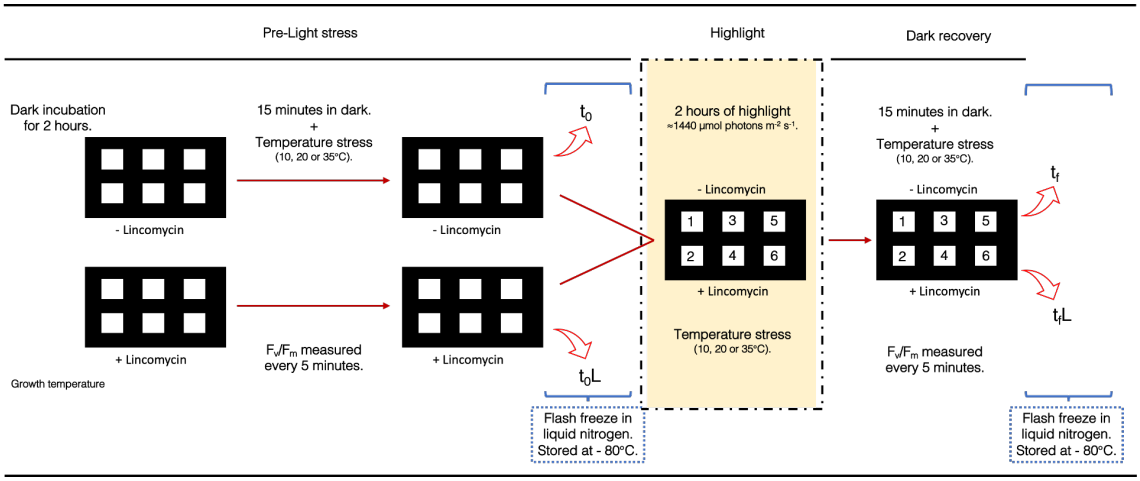

Figure 4 | Schematics of the experiment workflow for posterior quantitative analysis of the D1 protein by western blot. Two different time points were used t_0 and t_f. All samples were incubated in dark for two hours in the presence or absence of the protein inhibitor. After incubation period, samples were exposed at different temperatures, 10, 20 or 35 °C, for 15 minutes in dark, and were immediately flash freeze (t_0 and t_{0L}). The t_f and t_{fL} samples, were further exposed to a high light treatment for two hours, followed by 15 minutes in dark for recovery and immediately flash freeze. See Table 1 for notation.

2.3.3 Photoprotection capacity

The photoprotection capacity of *Bryopsis hypnoides* was estimated for each temperature by quantifying the recovery of $\Delta F/F_m'$ following the prolonged exposure to supersaturating irradiance, on the untreated samples used in the light stress-recovery protocol described above. The value of F_v/F_m (% of pre-stress level) reached after 15 min of recovery in the dark was used to estimate q_E, the energy-dependent component of NPQ (Müller et al., 2001).

2.4 Photoacclimation state

The photoacclimation state of the samples was characterized by measuring the light-response curves (LC) of the relative electron transport rate of PSII and of the nonphotochemical quenching index (rETR and Y(NPQ)), respectively; see Table 1 for notation). Light-response curves were generated at 20 °C by sequentially exposing each sample to 8 levels of actinic irradiance, up to 468 µmol photons m^{-2} s^{-1}. The sample was then exposed to the same *E* levels, but applied in the reverse order, generating a so-called 'hysteresis light curve'. The samples were exposed to each light level for 2 min after which a saturation pulse was applied and the fluorescence levels F_s and F_m' (steady state and maximum fluorescence of a light-adapted sample, respectively) were recorded. For each irradiance level, *E,* rETR was calculated from the product of *E* and the PSII effective quantum yield, $\Delta F/F_m'$ (Genty et al., 1989):

$$rETR = E\ \frac{F_m' - F_s}{F_m'} \qquad (3)$$

rETR vs *E* curves (ascending and descending, separately) were quantitatively described by fitting the model of Eilers & Peeters (1988) and by estimating the parameters α (the initial slope of the curve), $rETR_m$ (maximum rETR), and E_k (the light saturation, or photoacclimation, parameter). Hysteresis light-response curves of Y(NPQ) were also described by fitting the model of Serôdio & Lavaud (2011) (except for the descending values, since the model was not applicable for them) and by estimating the parameters $Y(NPQ_m)$ (the maximum

Y(NPQ) value reached), E_{50} (irradiance corresponding to 50% of NPQ_m) and n (sigmoidicity coefficient).Y(NPQ) quantifies the fate of excitation energy in PSII (Klughammer & Schreiber, 2008), calculated for each *E* level by:

$$Y(NPQ) = \frac{F}{Fm'} - \frac{F}{Fm} \quad (4).$$

Effects on the mean values of the various parameters were tested using one-ANOVA and by post hoc Tukey HSD test. Assumptions of normality and homoscedasticity were verified prior to analysis using the Shapiro–Wilk test and Levene's test, respectively. In case of violation of assumptions, data were log transformed. All statistical analyses were carried out using GraphPad Prism (GraphPad software SanDiego, USA).

Table 1 – Notation.

α	The initial slope of the *rETR* versus *E* curve (µmol photons $m^{-2}s^{-1}$)
E	PAR irradiance (umol photons $m^{-2}s^{-1}$)
E_k	Light-saturation parameter of the *rETR* versus *E* curve (µmol photons $m^{-2}s^{-1}$)
E_{50}	Irradiance level corresponding to 50% of NPQ_m in an NPQ versus *E* curve
rETR	PSII relative electron transport rate
$rETR_m$	Maximum *rETR* in a *rETR* versus *E* curve
F_o, F_m	Minimum and maximum fluorescence of a dark-adapted sample
F_s, $F_{m'}$	Steady-state and maximum fluorescence of a light-adapted sample
F_v/F_m	Maximum quantum yield of PSII
LC	Light-response curve
$Y(NPQ)_m$	Maximum *Y(NPQ)* value reached in a *Y(NPQ)* versus E curve
n	Sigmoidicity coefficient of the NPQ versus *E* curve
PSII	Photosystem II
t_0, t_0L	Time points before highlight stress, L denotes presence of lincomycin
t_f, t_fL	Time points after highlight and recovery in dark, L denotes presence of lincomycin

2.5 Protein extraction

The samples selected for extraction were those tested at 10, 20, and 35 °C. For protein extraction, algae were ground into a fine powder using a pestle and a mortar and liquid nitrogen. The powder was then transferred into 1.5 mL tubes at 4 °C, and 1 mL of extraction buffer (Table 2) was added. Cellular debris was removed by centrifugation (15,000×g, 7 min, 4 °C), and the supernatant was discarded. After, the protein pellet was resuspended in 500 µL isolation buffer (Table 2) and was vortex for complete protein solubilization. In the end, 5 aliquots were made for each sample and then kept at – 80 °C.

Table 2 - Protein extraction buffers.

Extraction buffer	Monopotassium phosphate	50 mM
	Protease Inhibitor (Sigma-Aldrich®)	1 mL
Isolation buffer	Tricine/KOH (pH 7.8)	0.952 mM
	Magnesium chloride hexahydrate	0.551 mM
	Sodium chloride	0.496 mM

2.6 Protein quantification

For each sample, protein concentration was measured in triplicate via Pierce™ BCA Protein Assay Kit (Thermo Scientific). Quantification protocol was followed according to the manufacturer's instructions.

2.7 Western blot

Western blot is widely used for protein identification. Western blotting consists in the separation of a mixture of proteins by polyacrylamide gel electrophoresis (PAGE) based on molecular weight (Hnasko & Hnasko, 2015) and posterior identification by a specific antibody. After the gel separation phase, proteins are transferred to a membrane. This process is also known as blotting. Blotting allows the fixation of the proteins, in a membrane ready for antibody labelling (Mahmood & Yang, 2012). Membranes are incubated with antibodies specific to the protein of interest and later, membranes are developed by proper solution (e.g., ECL for luminescence signal) (Fowler, 1995). During incubation, membranes are blocked to avoid unspecific binding of the antibodies to the membrane. Thus, antibodies bind specifically to the protein of interest, which should be the only one visible. The intensity of the bands observed is proportional to the amount of protein present. Using known quantities of the protein of interest it is possible to determine the quantity of protein present in samples. D1 quantity was normalized to the total protein concentration of each sample.

2.7.1 Sample preparation

Samples were diluted (5:1) in adding 6x Laemmli SDS sample buffer solution (Table 3) and vortexed. After, they are heated at 100 °C for 5 minutes, and cooled down at room temperature, after cooling they were again, briefly vortexed, and finally were given a quick spin down.

Table 3 – Laemmli SDS sample buffer.

Denaturing Solution		
6x (Six times concentrated)		Per 20 mL
	Sodium dodecyl sulfate (SDS)	2.4 g
	Bromophenol blue	0.001 g
	Tris (pH 6.8)	0.5 M
	Glycerol	9.4 mL
	dH_2O	4.2 mL
		Per aliquot
	ß-mercaptoethanol	9%

2.7.2 Gel electrophoresis

Samples were separated by SDS-PAGE according to Laemmli (1970). An electric field is applied that causes the negatively charged molecules to move. Polyacrylamide gels are used for protein separation and the method is therefore called Polyacrylamide gel electrophoresis (PAGE). For denaturing conditions, sodium dodecyl sulfate (SDS) is added to the system. The denaturing condition is essentially the unfold of tertiary structures into secondary structures generating an SDS-protein complex (Schägger, 2006) that yields a negative charge causing proteins to migrate towards the positive pole during electrophoresis (T. S. Hnasko & Hnasko, 2015), thus separating them by their molecular weights. The gel consists of two sections with different densities and pH values: (i) a stacking gel (Table 4), and (ii) a running gel (Table 4). All electrophoretic equipment should be thoroughly washed prior to use. Glass plates should be cleaned with ethanol and wiped dry with paper wipes.

Tetramethylethylenediamine (TEMED) and ammonium persulfate (APS) solutions, were added immediately before pouring the gel solution into the glass plates chamber, as they act as a catalyst for acrylamide gel polymerization. The running gel (4 mL) polymerized for 30 minutes covered with isopropanol (50% v/v). Isopropanol avoids the inhibition of the polymerization by oxygen and helps to make the border between the stacking and the resolving gel sharper.

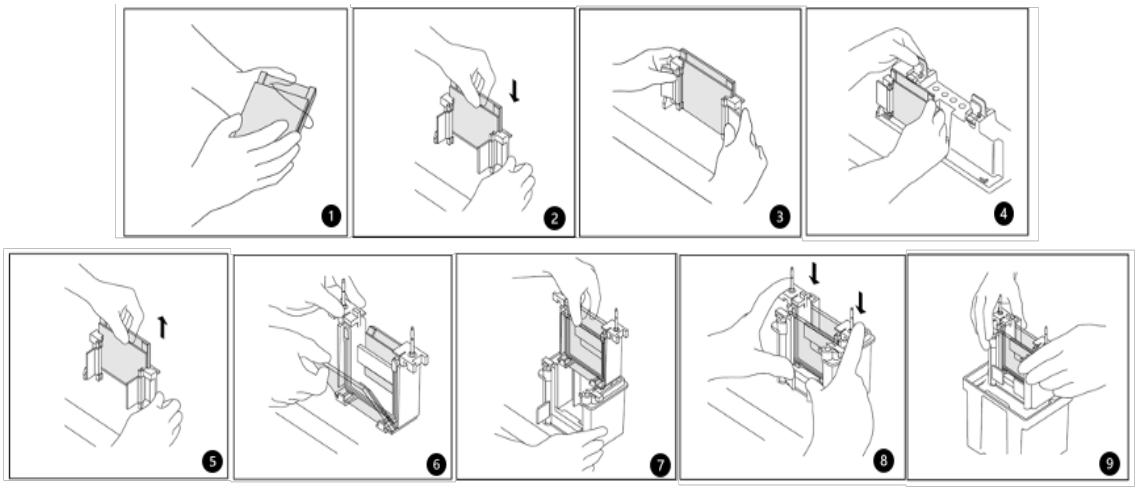

Figure 5 | Gel cassette preparation. Assembly steps follow crescent number order. Adapted from Bio-Rad Mini-PROTEAN® 3 Cell Assembly Guide.

For the stacking gel, the process was repeated, and before pouring it on top of the running gel, the isopropanol layer was removed. Then the 10 well comb was added, carefully, making sure there were no air bubbles between the gel and the comb. After gel polymerization, the electrophoresis chamber is filled with the running buffer (Table 5). Samples and the molecular weight marker were loaded into the gel with the help of a syringe (Hamilton). Electrophoresis occurred under a potential difference of 120v for 120 minutes. Electrophoresis was conducted in a Mini-Protean® 3 Cell (Bio-Rad) (Fig. 5) and a power supply PowerPac 300 (Bio-Rad).

Table 4 – SDS-PAGE Gels.

15 % SDS-Gel		
Running gel		For two gels
	Milli-Q water	3.26 mL
	40% 29:1 Acrylamide/ bis-Acrylamide (w/v)	5.00 mL
	1.5M Tris (pH 8.8)	2.52 mL
	10% SDS (w/v)	0.10 mL
	TEMED	0.004 mL
	10% Ammonium persulfate (APS) (w/v)	0.10 mL
Stacking gel		For two gels
	Milli-Q water	1.70 mL
	12M Urea	1.70 mL
	29:1 Acrylamide/ bis-Acrylamide	0.83 mL
	1M Tris (pH 6.8)	0.63 mL
	10% SDS (w/v)	0.05 mL
	TEMED	0.005 mL
	10% APS (w/v)	0.05 mL

Table 5 – SDS-PAGE running buffer.

Running buffer		
5x (five times concentrated)		
	Tris	15.1 g
	Glycine	94.0 g
	10 % SDS (w/v)	50.0 mL
1x	Running buffer 5x	200 mL

2.7.3 Transfer

For protein transfer, Immun-Blot™ PVDF membranes (Bio-Rad) were used. The membrane was activated in methanol and equilibrated in transfer buffer (Towbin et al., 1979) (Table 6) for 5 minutes. Filter papers, and sponges were also equilibrated in transfer buffer. PVDF membranes were found to be the best for D1 protein due to their hydrophobicity. All the equipment was cleaned with distilled water prior to use

The transfer buffer was made prior to use, and methanol was added immediately before use. During the course of this work, it was realized that using ice cold transfer buffer improved transfer quality.

Blotting was carried out in a Mini Trans-Blot® Electrophoretic Transfer Cell (Bio-Rad) apparatus (Fig. 6) linked to a power supply PowerPac 300 (Bio-Rad) for 210 minutes under a constant electric current of 150 mA, at 4°C.

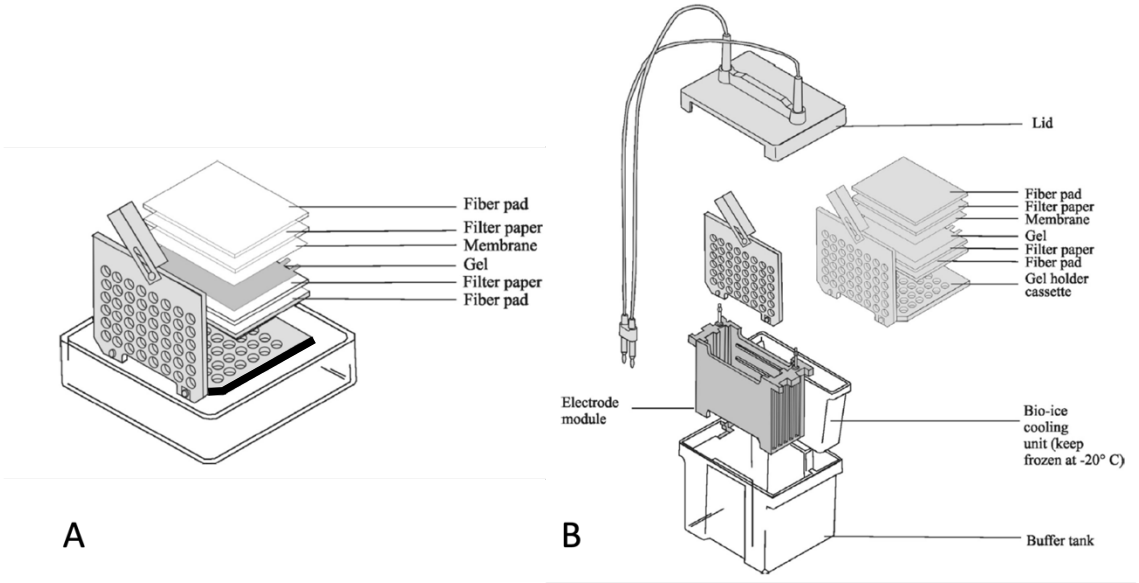

Figure 6 | Sandwich assembly for wet transfer **(A)** and preparation for protein transfer using the Mini-Trans-blot apparatus **(B).** Adapted from Kurien & Scofield, 2019.

2.7.4 Protein detection

After blotting, membranes were washed in TTBS (Table 7) for three minutes and incubated with 25 mL of 1% blocking buffer (Table 8) for 1h at room temperature. To control transfer quality, any remaining proteins on the gels were

stained with Coomassie brilliant blue R-250 (Table 9) for 30-40 minutes and destained overnight.

Table 6 – Towbin buffer with SDS.

Transfer buffer (pH 8.3)		
	Tris	192 mM
	Glycine	25 mM
	SDS (w/v)	0.1 %
	Methanol	20 %

The blocking buffer was then replaced for the primary antibody solution (Table 10) and incubated at 4 °C, overnight, under slight agitation. Afterwards, primary antibody solution was decanted, the membrane was washed in TTBS for 10 minutes, at room temperature on a shaker and incubated with the secondary antibody solution, for one hour, at room temperature under mild agitation.

After incubation, membranes were washed 4 times in TTBS for 5 minutes each. The washing step allows the removal of background improving detection quality.

For the detection, 1 mL of ECL solution (Table 11) was added to the membranes and developed for 60 seconds. Detection was made using ChemiDoc™ XRS+ Molecular Imager® (Bio-Rad) and later analyzed with the ImageLab software (Bio-Rad).

Table 7 – Tris buffered saline.

TTBS		
		Per litre
	Tris	2.4 g
	NaCl	29.2 g
	Tween 20	0.5 mL

Table 8 – Blocking buffer.

	TTBS	50.0 mL
	Skimmed milk powder	0.5 g

Table 9 – Staining and destaning solutions.

Coomassie brilliant blue R-250	Methanol	45 %
	Glacial acetic acid	10 %
	Coomassie brilliant blue R-250	3.0 g/L
Destain solution	Ethanol	25 %
	Glacial acetic acid	5 %

Table 10 – Antibody solutions.

Primary antibody solution	Blocking buffer	25.0 mL
	Rabbit anti-PsbA|D1 Protein of *PSII* (Agrisera)	5.0 uL
Secondary antibody solution	Blocking buffer	25.0 mL
	Goat anti-Rabbit IgG (Agrisera)	5.0 uL

Table 11 – Enhanced chemiluminescence (ECL) reagents

ECL		
Solution A		Per 250 mL
	Luminol (in DMSO)	0.1 mM
	4-iodophenol (in DMSO)	2.0 mM
	0.1 M Tris (pH 9.35)	50.0 mM
Solution B		
	3 % Hydrogen Peroxide	
Prepare immediately prior to use	A/B (100/1, v/v)	

3. Results

3.1. Variation of K_{PI} and K_{REC} with temperature

Figure 7 shows the variation of the maximum quantum yield of PSII, F_v/F_m, before and after the exposure to supersaturating irradiance of 1440 µmol photons m^{-2} s^{-1} during 120 minutes of samples to temperatures ranging between 5-35 ^oC, in the absence or presence of the lincomycin.

For all temperatures, pre-stress F_v/F_m values remained constant until the start of the light exposure, both in control and lincomycin-treated samples. Following light exposure, F_v/F_m were substantially decreased and, in most cases, recovered partially during the first 15 minutes (Fig. 7A-D). However, in the extreme case of 35 ^oC, F_v/F_m did not show signs of recovery and the values decreased slightly (Fig. 7E). The lower temperatures tested, 5 and 10 °C (Figs. 7A and 7B, respectively), caused the largest effects on the decrease and recovery in F_v/F_m, when compared to the effects observed under the growth temperature (20 ^oC). For both temperatures, the recovery after light stress reached only 15% of pre-stress levels, with hardly any differences between controls and lincomycin-treated samples. At 20 ^oC (Fig. 7C), the control algae (measured as F_v/F_m in the absence of the lincomycin), showed a recovery of 45%, and a significant effect of lincomycin was evident, with lincomycin-treated samples recovering only to 30% of pre-stress levels. The increase of the temperature to 25°C was well tolerated by the algae (Fig. 7D), with a small difference of 10 % in the presence of lincomycin at the end of the experiment, comparing to the exposure to 20 °C. Nevertheless, in the control group, a significant drop of the recovery capacity could be observed, from 45% to approximately 33%. At the highest temperature tested, 35 °C, the algae reached the lowest percentage of recovery both in the absence and presence of the inhibitor (Fig. 7E), reaching less than 15% in the control samples and less than 10% recovery in the lincomycin-treated ones. These results are summarized in Figure 8, highlighting the invariance of pre-stress F_v/F_m with temperature and the marked effects light stress, as shown in $\%F_v/F_m$.

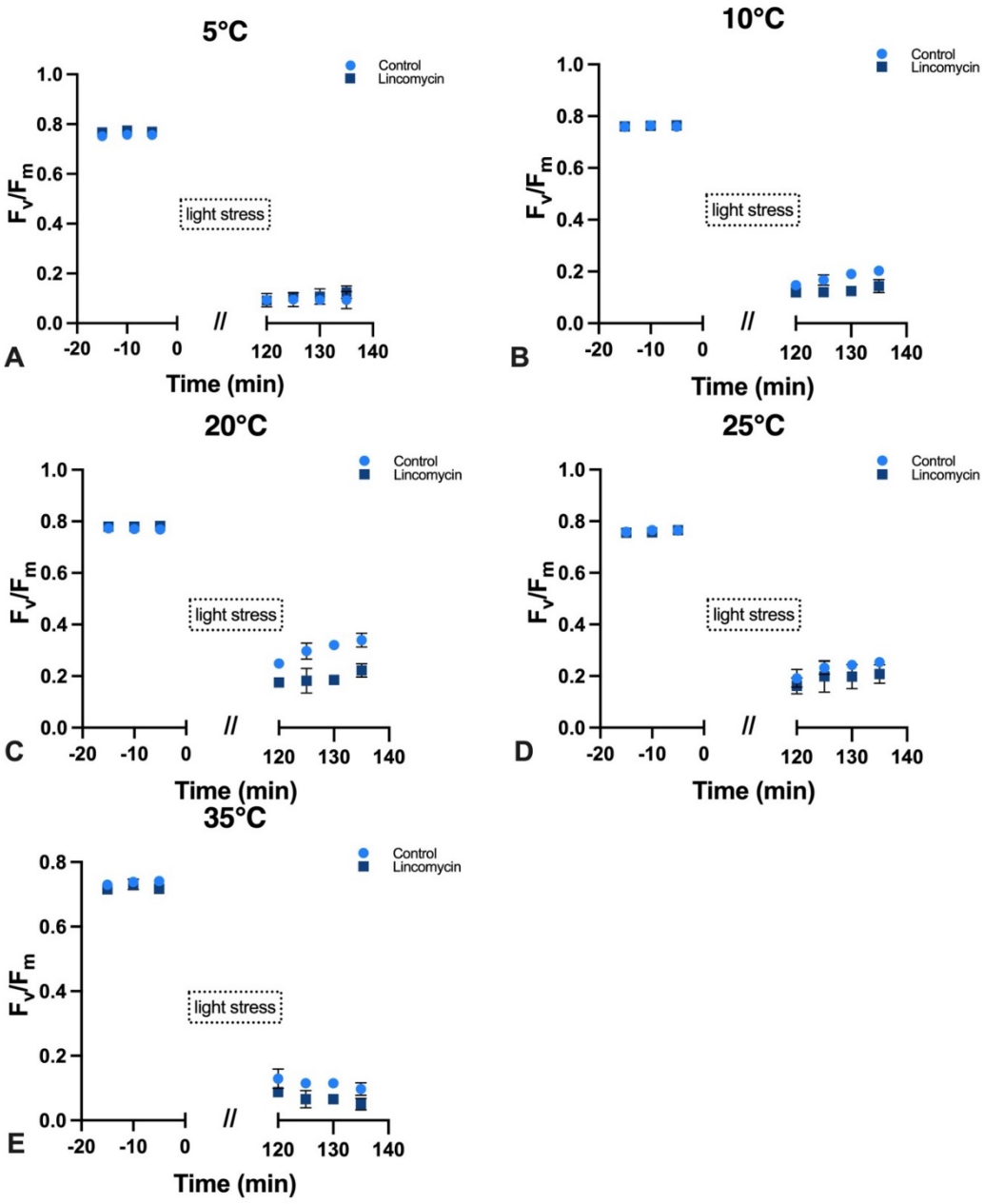

Figure 7 | Variation of F_v/F_m over time, between pre-light stress and recovery in dark at 5 temperatures, in the absence or presence of lincomycin (light-blue circles or dark-blue squares, respectively). F_v/F_m values were measured at 5°C **(A)**, 10°C **(B)**, 20°C **(C)**, 25°C **(D)** and 35°C **(E)**. All measurements were performed in biological triplicates and error bars indicate one standard deviation.

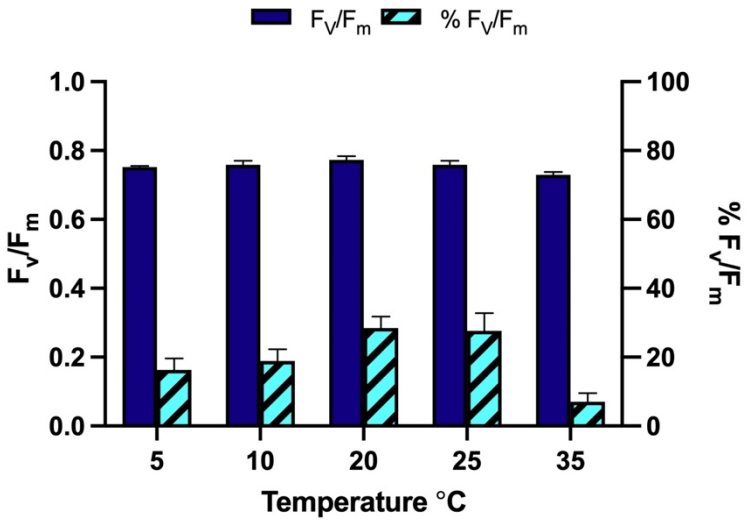

Figure 8 | Variation of F_v/F_m (pre-stress) and $\%F_v/F_m$ with temperature. All measurements were performed in biological triplicates and error bars represents one standard deviation.

The rate constant of PSII photoinactivation, k_{PI}, showed an asymmetrical response to changes in temperature. The lowest value, of 1.73×10^{-4} s^{-1}, was measured under growth temperature (20 °C) (Fig. 9). Higher and lower temperatures caused an increase in k_{PI}, but the highest temperature tested, 35 °C, caused a larger increase in k_{PI}, than the temperatures below growth temperature, 5 and 10 °C (Fig. 9). Maximum values reached 3.65×10^{-4} s^{-1}, measured for 35 °C, representing an increase of 111% relatively to 20 °C.

The rate constant of repair of photoinactivated PSII, k_{REC}, also varied markedly with temperature, but showing a pattern opposed to the one of k_{PI} (Fig. 10). Maximum values, of 1.34×10^{-4} s^{-1}, were measured for 20 °C, decreasing as temperature was lowered or increased. The capacity of repair decreased markedly with both low and high temperatures, reaching the lowest values of 0.36×10^{-4} s^{-1} for 5 °C. In all cases, k_{REC} was lower than k_{PI}, the smaller difference between the two being observed for 20 °C.

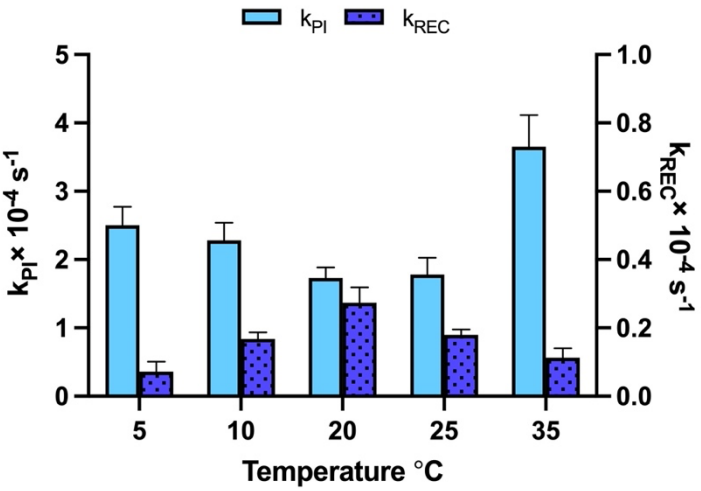

Figure 9 | Variation of the rate constants of photoinactivation, k_{PI}, with temperature, and variation of recovery of inactivated PSII, k_{REC}, opposed to k_{PI}. All measurements were performed in biological triplicates and error bars represents one standard deviation.

The variation of the NPQ index q_E, indicative of the photoprotective capacity, also responded to temperature, following closely the patterns displayed by k_{REC} (Fig. 9). Maximum values were observed for 20 °C, decreasing with lower and higher temperatures. q_E (Fig. 10) was found to correlate significantly with k_{REC} (r^2 = 0.948, p-value < 0.05).

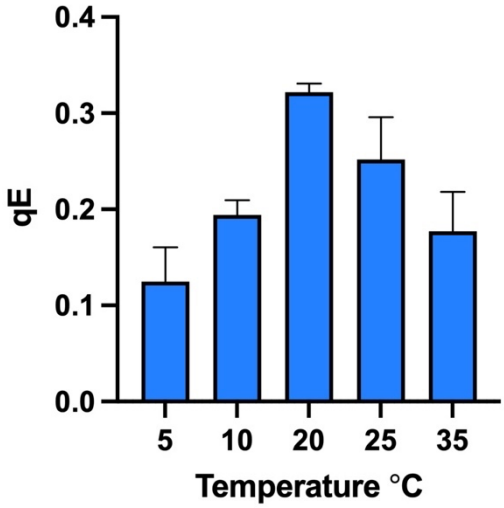

Figure 10 | Variation of energy-dependent non-photochemical quenching index, qE, with temperature. All measurements were performed in biological triplicates and error bars represent one standard deviation.

3.2. Hysteresis light-response curves

Figure 11 shows the results of the hysteresis light-response curves for rETR and Y(NPQ). Tables 12 and 13 show the average values of the parameters of the models fitted to rETR and Y(NPQ) light curves.

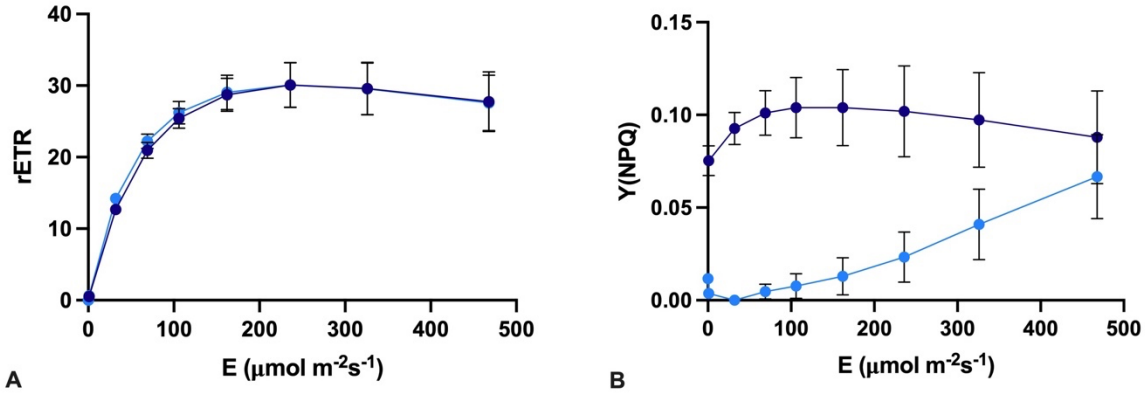

Figure 11 | Hysteresis light-response curves of *PSII* relative electron transport rate, rETR **(A)** and non-photochemical quenching index yield Y(NPQ) **(B)**. Ascending curves in light blue and descending curves in dark blue. All measurements were performed in biological triplicates and error bars represent one standard deviation.

In the case of rETR (Fig. 11A), the light response was characterized by the reaching of a saturation for relatively low irradiance values, with E_k parameter varying between 47.6 and 58.1 µmol m^{-2} s^{-1}. The light-ascending and light-descending curves did not differ substantially. In contrast, the light-response curves of Y(NPQ) showed a marked difference between light-increasing and light-decreasing parts of the hysteresis curve (Fig. 11B). During the light-increase phase, Y(NPQ) increased as expected, but when applied irradiance was decreased, Y(NPQ) continued to increase during several light steps, until it started to decrease, only for light levels around 160 µmol m^{-2} s^{-1} (Fig. 11B). Due this sustained response of Y(NPQ), the model of Serôdio & Lavaud (2011) could not be used for the light-descending part of the light curve and the parameters values are not shown in Table 13.

Table 12 – rETR light-response curve parameters (α, $rETR_m$ and E_k) for the light- increasing and light-decreasing parts of the LC.

	α	$rETR_m$	E_k
Ascending	0,633	30,099	47,631
Descending	0,529	30,232	58,170

Table 13 – Y(NPQ) light-response curve parameters ($Y(NPQ_m)$, E_{50} and n) for the light- increasing part of the LC.

	$Y(NPQ_m)$	E_{50}	n
Ascending	0,29	934,53	2,01

3.3. D1 protein quantification and response to temperature

D1 was quantified by western blot, at two different time points t_0 and t_f. A standard curve with pure D1 protein (Fig. 12) was built for comparison purposes.

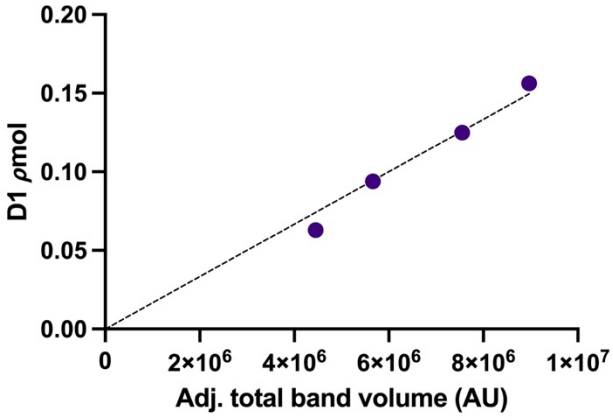

Figure 12 | D1 protein of Photosystem II standard curve obtained by quantification of the D1 immunoblot signal (Adjusted total band volume in arbitrary units). PsbA|D1 protein of PSII positive control/quantitation standard (Agrisera).

D1 quantity at t_0, for all samples was very low (Fig. 13A). Samples exposed to the inhibitor at the 35 °C showed a slight increase on the D1 concentration. At the end of the experiment, t_f, D1 concentration increased at all temperatures. The highest D1 concentration was detected at 20°C (0.0019 pmol ug^{-1}). Furthermore, at 20 °C, there is a clear difference between the D1 concentration in algae incubated in the absence or presence of lincomycin. In average the presence of lincomycin lead to a reduction of D1 concentration at the end of the experiment (Fig. 13B). Nonetheless, at 10 °C and 35 °C, the inhibitor's effect was marginal. This outcome may be related to the temperature itself, as the cold and heat stresses might influence the inhibitor mechanism of action.

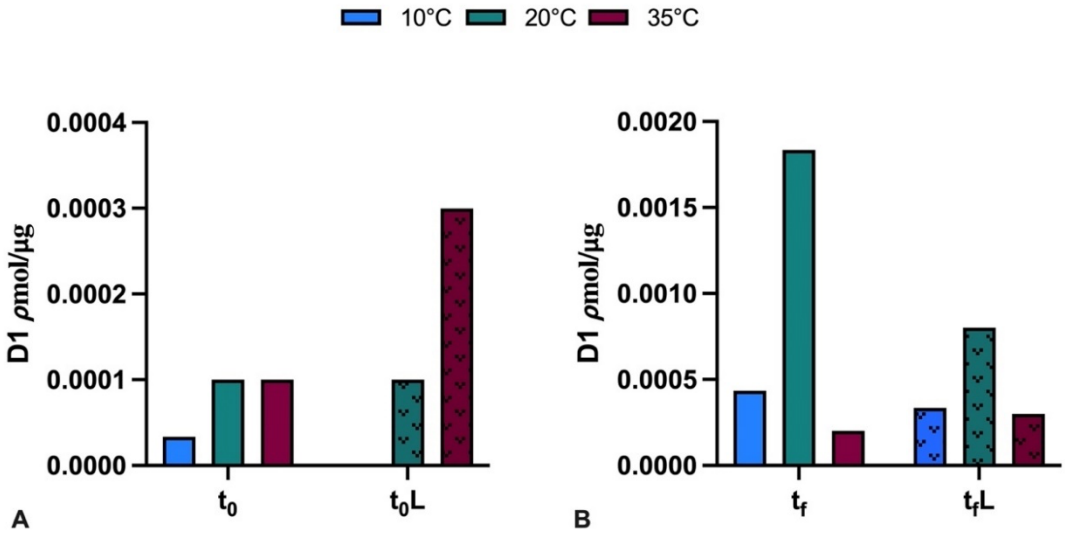

Figure 13 | Samples D1 concentration in the beginning and at the end of the experiment (t_0, t_{0L} and t_f, t_{fL}, respectively) in the presence or absence of lincomycin (columns with and without pattern, respectively) at the different temperatures.

The D1 quantity ratio, from samples exposed to lincomycin was found to co-vary linearly with $\%F_v/F_m$ (Fig. 14), for the different temperatures. There's little disparity when comparing the highest and lowest temperatures, both contrast with the D1 at 20 °C, close to the growth temperature.

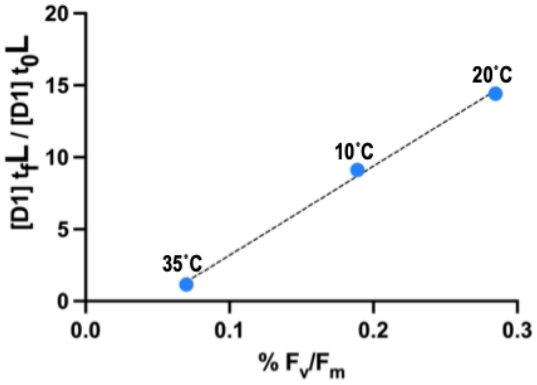

Figure 14 | D1 concentration ratio (t_{fL} /t_{0L}) after highlight treatment obtained by quantification of the D1 immunoblot signal, normalized by the total protein content, in the presence of lincomycin, compared to the percentage of F_v/F_m recovery under the different temperatures.

4. Discussion

4.1. Effects of temperature on PSII photoinactivation and repair

The results based on the *in vivo* Chl fluorescence index $\%F_v/F_m$ have shown marked effects of both low and high temperatures on the PSII inactivation and repair processes, by showing a decrease on the post-light stress F_v/F_m recovery in both control and lincomycin-treated samples. Although both the cold and moderate heat conditions tested in the study caused clear negative effects in $\%F_v/F_m$, high temperatures induced a larger decrease in $\%F_v/F_m$ when compared to lower temperatures, denoting a higher susceptibility of the *Bryopsis hypnoides* metabolism to heat than to cold conditions.

Significant light-induced effects on PSII were quantified by the large rate constants of PSII, k_{PI}, that were measured on lincomycin-treated samples. Both high and low temperatures induced the increase of k_{PI}, meaning that both cold and heat stress have a direct effect on PSII photoinactivation. Our data showed an asymmetrical response, with higher temperatures caused a larger increase while low temperatures had a lighter effect. Temperature effects on the repair of photoinactivated PSII were detected by the exacerbated light-induced decreases in lincomycin-treated samples than on control samples.

The temperature dependence of the repair of inactivated PSII has been suggested to be related to a higher sensitivity to photoinhibition at lower temperatures (Tsonev & Hikosaka, 2003). The repair maximum rate decreases when, under cold stress, inhibition of protein synthesis by low temperatures slows down D1 protein degradation as well as processing of its precursor pre-D1 (Nishiyama & Murata, 2014). In tomato leaves, low temperature associated with highlight exposure, interferes with degradation and removal of damaged D1 from the reaction center during the repair process (Grennan & Ort, 2007). Inactivation and repair processes are both suppressed at low temperature however its effects are more significative in the inactivation process and consequential photoinhibition is enhanced when compared to high temperature (Gombos et al., 1994). Thylakoid membrane biogenesis and quality control of its proteins are mainly described as dependent on *ftsH* protease (Kato & Sakamoto, 2018). Evidence shows that low temperature induced stress inhibits D1 protein proteolytic degradation by *ftsH* as well as pre-D1 processing (Nishiyama & Murata, 2014). Although, *ftsH* gene is absent on *Bryopsis hypnoides* chloroplast genome (Leliaert & Lopez-Bautista, 2015; Lü, Xü, et al., 2011b), D1 protein degradation still occurs. However, the lack

of studies regarding protection mechanisms on this alga makes the distinction of the affected steps by abiotic stress a difficult task.

On the other hand, moderate heat stress is known to enhance net photoinhibition (Allakhverdiev et al., 2007; Nishiyama & Murata, 2014). In cyanobacteria, the CO_2 fixation process is sensitive to moderate heat stress, which represses the repair of PSII thus enhancing photoinhibition (Allakhverdiev et al., 2007). This is because the limited supply of the CO_2 fixation process inhibits chloroplast protein synthesis (Takahashi & Murata, 2006). In the present study, a moderate heat stress, such as 35°C, caused a larger increase in k_{PI} than the effect seen at the lower temperatures, which may indicate a direct effect of the heat stress.

The PSII repair capacity, as measured by the rate constants of repair of the inactivated PSII, k_{REC}, was also impacted by both low and high temperatures. As with k_{PI}, an asymmetrical response was observed, with heat stress causing a larger effect than the cold stress. Even though, for all temperatures, k_{PI} was higher than the corresponding k_{REC}, and larger temperature-induced changes were in general observed for k_{REC} than for k_{PI}. This may be due to the high irradiance that was applied, as k_{REC} is known to saturate for relatively low irradiance levels. Other studies with low-light adapted samples had similar responses regarding k_{REC} and k_{PI}, meaning that photoinactivation rates exceeded the repair rates when exposed to substantially higher irradiances than the growth irradiance (Serôdio et al., 2017).

4.2. Effects of thermal stress on light-induced loss of D1 content

Our results also evidence the efficacy of the chloroplast-encoded protein inhibitor to reduce the capacity of the repair and synthesis *de novo* of the D1 protein. Regardless, other factors should be considered when addressing the repair capacity of the PSII.

There is a well-known relationship between light intensity and the repair metabolism. In *Spirodela oligorhiza*, the rate of a 32 kDa protein synthesis, is related to the intensity of light (Matto et al, 1984). Light is required for the functional recovery of PSII. When under highlight, damage to PSII and repair of the damaged PSII, are processes occurring concomitantly (Aro et al., 1994).

Aro et al. (1993a) described the recovery process as follows: (1) proteolytic degradation of the damaged D1 protein, (2) total removal of the degraded D1 protein, (3) synthesis of the D1 protein precursor, (4) processing of the precursor

protein, (5) insertion of the new D1 protein into the PSII to restore its photochemical activity.

Mattoo et al. (1984), performed an experiment following radiolabeled membrane proteins of white and dark-adapted green fronds of *Spirodela oligorhiz*a. At time 0 (*i.e.*, no illumination time after a dark incubation period) there was no 32-kDa (authors termed it 32 kDa protein), D1 protein band. One hour after being in light exposure, the 32-kDa protein band was present suggesting that D1 synthesis is light related. In the present study, all samples were grown under low light, and for the experiment were later incubated for two hours in complete darkness. On the western blot analysis, D1 protein concentration detected in the t_0 samples was very low. We can hypothesize that in dark D1 synthesis is reduced, similarly to what happened in the study of Mattoo et al. (1984). Answering this question is beyond the scope of this study, but data here presented provides some support for this hypothesis.

There's little disparity when comparing the highest and lowest temperatures, both contrast with the D1 concentration, 0.0019 pmol/ug, at 20 °C, closest to the growth temperature. We may infer that such extreme temperatures induce a perturbation of the repair mechanisms. By the end of the experiment, the amount of D1 protein appears to increase, which is likely that refers to a precursor form to D1, and that in the recovery period it should disappear to give way to the final form of D1, similarly to what is described by Kettunen et al. (1991). There is a high possibility that the time the alga was in the dark for recovery (15 minutes), after the light exposure, was not enough for the protein to be completely degraded. For example, Kettunen et al. (1991) left intact pumpkin leaves in recovery conditions for 24 hours. The precursor/modified form of the D1, together with the protein that was not degraded or that simply did not enter the repair cycle, suggests that the amount of D1 protein increased with exposure to light

4.3. The ‘new paradigm’ in XC-deficient Bryopsidales

As an algal fitness indicator widely-used in physiological studies, the maximum quantum efficiency of PSII, F_v/F_m, is often assumed, often without experimental validation, to be a reliable proxy for photoinhibitory effects caused by abiotic stress (Eggert et al., 2007). The very strong correlation observed in this study between $\%F_v/F_m$ and the relative D1 protein content confirms the validity of the fluorescence index to track light-induced short-term changes in D1 content.

Both types of parameters, $\%F_v/F_m$ and D1 content concur in showing that abiotic stress, in this case cold and moderate heat, have a negative impact on PSII photoinactivation in *Bryopsis hypnoides*. These results have direct implications for the validation of the general validity of the 'new paradigm' of photoinhibition: it does not seem to hold in this as cold and moderate heat were shown to affect net photoinhibition not just by decreasing the PSII repair capacity but by directly increasing PSII inactivation. For most temperatures tested, the effects were larger for repair than for photoinactivation, but the two were comparable in magnitude, not supporting the main claim of the hypothesis.

This may be due to the lack of a functional xanthophyll cycle in *Bryopsis hypnoides*, an efficient photoprotective mechanism that would otherwise alleviate the impact of light-induced ROS on D1 photoinactivation. A corollary of the new paradigm is that photoprotective mechanisms like NPQ act primarily not by preempting PSII photoinactivation per se but by protecting the PSII repair process from ROS inhibition (Murata et al. 2012). As an indication of the photoprotective capacity of PSII, q_E was calculated for the different temperatures tested. q_E quantifies the excessive light energy that is dissipated as thermal energy by the photoprotective response mechanisms (Tokutsu et al., 2019). Cold stress had a larger effect than the heat stress, meaning that the protective capacity was strongly limited by low temperatures. q_E was seen to correlate with k_{REC}, which can be interpreted as an indication that thermal stress limits the photoprotection capacity and the repair capacity in the same way. An inverse relationship between q_E and suffered photoinactivation, k_{PI}, was also observed, possibly denoting that the loss in photoprotection capacity may be in the origin of the increase in PSII photoinactivation.

To conclude, the deficiency in XC and q_E in the group of algae, Bryopsidales, is a recent discovery and should be used as the grounds for further investigation. Furthermore, for future evolutionary studies, Ulvophyceae is a rich and diverse family and should be considered for this purpose (Christa et al., 2017). In addition, this family can also be considered as the subject of photoprotection mechanisms investigation and genomic studies with the purpose of enlightening this particular subject within the scope of photophysiology (Handrich et al., 2017).

5. References

Allakhverdiev, S. I., Los, D. A., Mohanty, P., Nishiyama, Y., & Murata, N. (2007). Glycinebetaine alleviates the inhibitory effect of moderate heat stress on the repair of photosystem II during photoinhibition. *Biochimica et Biophysica Acta - Bioenergetics*, *1767*(12), 1363–1371. https://doi.org/10.1016/j.bbabio.2007.10.005

Armbruster, U., Zühlke, J., Rengstl, B., Kreller, R., Makarenko, E., Rühle, T., Schünemann, D., Jahns, P., Weisshaar, B., Nickelsen, J., & Leistera, D. (2010). The *arabidopsis* thylakoid protein PAM68 is required for efficient D1 biogenesis and photosystem II assembly. *Plant Cell*, *22*(10), 3439–3460. https://doi.org/10.1105/tpc.110.077453

Aro, E. M., Virgin, I., & Andersson, B. (1993a). Photoinhibition of photosystem II. Inactivation, protein damage and turnover. *Biochimica et Biophysica Acta - Bioenergetics*, *1143*(2), 113–134. https://doi.org/10.1016/0005-2728(93)90134-2

Aro, E. M., McCaffery, S., & Anderson, J. M. (1993b). Photoinhibition and D1 protein degradation in peas acclimated to different growth irradiances. *Plant Physiology*, *103*(3), 835–843. https://doi.org/10.1104/pp.103.3.835

Aro, E. M., McCaffery, S., & Anderson, J. M. (1994). Recovery from photoinhibition in peas (*Pisum sativum L.*) acclimated to varying growth irradiances: Role of D1 protein turnover. *Plant Physiology*, *104*(3), 1033–1041. https://doi.org/10.1104/pp.104.3.1033

Blokhina, O., Virolainen, E., & Fagerstedt, K. V. (2003). Antioxidants, oxidative damage and oxygen deprivation stress: A review. In *Annals of Botany* (Vol. 91, pp. 179–194). https://doi.org/10.1093/aob/mcf118

Campbell, D. A., & Tyystjärvi, E. (2012). Parameterization of photosystem II photoinactivation and repair. *Biochimica et Biophysica Acta - Bioenergetics*, *1817*(1), 258–265. https://doi.org/10.1016/j.bbabio.2011.04.010

Christa, G., Cruz, S., Jahns, P., de Vries, J., Cartaxana, P., Esteves, A. C., Serôdio, J., & Gould, S. B. (2017). Photoprotection in a monophyletic branch of chlorophyte algae is independent of energy-dependent quenching (qE). *New Phytologist*, *214*(3), 1132–1144. https://doi.org/10.1111/nph.14435

Christa, G., Pütz, L., Sickinger, C., Clavijo, J. M., Laetz, E. M. J., Greve, C., & Serôdio, J. (2018). Photoprotective non-photochemical quenching does not prevent kleptoplasts from net photoinactivation. *Frontiers in Ecology and Evolution*, *6*(AUG), 1–11. https://doi.org/10.3389/fevo.2018.00121

Davison, I. R. (1991). Environmental effects on algal photosynthensis. In *J. Phyc.* (Vol. 27, pp. 2–8).

Demmig-Adams, B., & Adams, W. W. (1996). The role of xanthophyll cycle carotenoids in the protection of photosynthesis. *Trends in Plant Science*, *1*(1), 21–26. https://doi.org/10.1016/S1360-1385(96)80019-7

Demmig-Adams, B., & Adams, W. W. (2016). Photoinhibition. *Encyclopedia of Applied Plant Sciences*, *1*, 78–85. https://doi.org/10.1016/B978-0-12-394807-6.00093-9

Eggert, A., Nitschke, U., West, J. A., Michalik, D., & Karsten, U. (2007). Acclimation of the intertidal red alga *Bangiopsis subsimplex* (Stylonematophyceae) to salinity changes. *Journal of Experimental Marine Biology and Ecology*, *343*(2), 176–186. https://doi.org/10.1016/j.jembe.2006.11.015

Eilers, P. H. C., & Peeters, J. C. H. (1988). A model for the relationship between light intensity and the rate of photosynthesis in phytoplankton. *Ecological Modelling*, *42*(3–4), 199–215. https://doi.org/10.1016/0304-3800(88)90057-9

Fowler, S. J. (1995). Use of monoclonal antibodies for western blotting with enhanced chemiluminescent detection. *Methods in Molecular Biology (Clifton, N.J.)*, *45*, 115–127. https://doi.org/10.1385/0-89603-308-2:115

Genty, B., Briantais, J. M., & Baker, N. R. (1989). The relationship between the quantum yield of photosynthetic electron transport and quenching of chlorophyll fluorescence. *Biochimica et Biophysica Acta - General Subjects*, *990*(1), 87–92. https://doi.org/10.1016/S0304-4165(89)80016-9

Giovagnetti, V., Han, G., Ware, M. A., Ungerer, P., Qin, X., Wang, W. Da, Kuang, T., Shen, J. R., & Ruban, A. V. (2018). A siphonous morphology affects light-harvesting modulation in the intertidal green macroalga *Bryopsis corticulans* (Ulvophyceae). *Planta*, *247*(6), 1293–1306. https://doi.org/10.1007/s00425-018-2854-5

Gombos, Z., Wada, H., & Murata, N. (1994). The recovery of photosynthesis from low-temperature photoinhibition is accelerated by the unsaturation of membrane lipids: A mechanism of chilling tolerance. *Proceedings of the National Academy of Sciences of the United States of America*, *91*(19), 8787–8791. https://doi.org/10.1073/pnas.91.19.8787

Goss, R., & Jakob, T. (2010). Regulation and function of xanthophyll cycle-dependent photoprotection in algae. In *Photosynthesis Research* (Vol. 106, Issues 1–2, pp. 103–122). https://doi.org/10.1007/s11120-010-9536-x

Goss, R., & Latowski, D. (2020). Lipid dependence of xanthophyll cycling in higher plants and algae. *Frontiers in Plant Science*, *11*. https://doi.org/10.3389/FPLS.2020.00455/FULL

Greer, D. H., Berry, J. A., & Bj6rkman, O. (1986). Photoinhibition of photosynthesis in intact bean leaves: role of light and temperature, and requirement for chloroplast-protein synthesis during recovery*. *Planta*, *168*, 253–260.

Grennan, A. K., & Ort, D. R. (2007). Cool temperatures interfere with D1 synthesis in tomato by causing ribosomal pausing. *Photosynthesis Research*, *94*(2–3), 375–385. https://doi.org/10.1007/s11120-007-9169-x

Guillard, R. R. L., & Ryther, J. H. (1962). Studies of marine planktonic diatoms. I. *Cyclotella nana hustedt*, and *Detonula confervacea* (CLEVE) . Canadian Journal of Microbiology 8:229-239. *Can. J. Microbiol.*, *8*(1140), 229–239.

Handrich, M., de Vries, J., Gould, S. B., Serôdio, J., & Christa, G. (2017). Ulvophyceaen photophysiology and research opportunities. *Perspectives in Phycology*, *4*(2), 83–92. https://doi.org/10.1127/pip/2017/0074

Henley, W. J., Major, K. M., & Hironaka, J. L. (2002). Response to salinity and heat stress in two halotolerant chlorophyte algae. *Journal of Phycology*, *38*(4), 757–766.

Herrmann, R. G., & Westhoff, P. (2001). Thylakoid biogenesis and dynamics: The result of a complex phylogenetic puzzle. In Eva-Mari Aro & B. Andersson (Eds.), *Regulation of Photosynthesis* (pp. 1–28). Springer Netherlands. https://doi.org/10.1007/0-306-48148-0_1

Hnasko, T. S., & Hnasko, R. M. (2015). The Western Blot. In R. Hnasko (Ed.), *ELISA. Methods in Molecular Biology* (Vol. 1318, pp. 87–96). Humana Press, New York, NY. https://doi.org/https://doi.org/10.1007/978-1-4939-2742-5_9

Kato, Y., & Sakamoto, W. (2018). FtsH protease in the thylakoid membrane: Physiological functions and the regulation of protease activity. *Frontiers in Plant Science*, *9*(June), 1–8. https://doi.org/10.3389/fpls.2018.00855

Kettunen, R., Tyystjärvi, E., & Aro, E. M. (1991). D1 protein degradation during photoinhibition of intact leaves a modification of the D1 protein precedes degradation. *FEBS Letters*, *290*(1–2), 153–156. https://doi.org/10.1016/0014-5793(91)81247-6

Klaff, P., & Gruissem, W. (1991). Changes in chloroplast mRNA stability during leaf development. *Plant Cell*, *3*(5), 517–529. https://doi.org/10.2307/3869357

Klughammer, C., & Schreiber, U. (2008). Complementary PS II quantum yields calculated from simple fluorescence parameters measured by PAM fluorometry and the saturation pulse method. *PAM Application Notes*, *1*(1), 27–35. http://www.walz.com/

Kok, B. (1956). On the inhibition of photosynthesis by intense light. *Biochimica et Biophysica Acta*, *21*(2), 234–244. https://doi.org/https://doi.org/10.1016/0006-3002(56)90003-8

Komenda, J. (2000). Role of two forms of the D1 protein in the recovery from photoinhibition of photosystem II in the cyanobacterium *Synechococcus PCC 7942*. *Biochimica et Biophysica Acta - Bioenergetics*, *1457*(3), 243–252. https://doi.org/10.1016/S0005-2728(00)00105-5

Kuebler, J. E., Davison, I. R., & Yarishi, C. (1991). Photosynthetic adaptation to temperature in the red algae *Lomentaria baileyana* and *Lomentaria orcadensis*. *British Phycological Journal*, *26*(1), 9–19. https://doi.org/10.1080/00071619100650021

Laemmli, U. K. (1970). Cleavage of structural proteins during the assembly of the head of bacteriophage T4. *Nature*, *227*(5259), 680–685. https://doi.org/10.1038/227680a0

Lam, D. W., & Zechman, F. W. (2006). Phylogenetic analyses of the bryopsidales (Ulvophyceae, Chlorophyta) based on RUBISCO large subunit gene sequences. *Journal of Phycology*, *42*(3), 669–678. https://doi.org/10.1111/j.1529-8817.2006.00230.x

Leliaert, F., & Lopez-Bautista, J. M. (2015). The chloroplast genomes of *Bryopsis plumosa* and *Tydemania expeditiones* (Bryopsidales, Chlorophyta): Compact genomes and genes of bacterial origin. *BMC Genomics*, *16*(1), 1–20. https://doi.org/10.1186/s12864-015-1418-3

Li, D., Lü, F., Wang, G., & Zhou, B. (2009). Assembly of the subcellular parts of *Bryopsis hypnoides* Lamouroux into new protoplasts. *Russian Journal of Plant Physiology*, *56*(1), 110–117. https://doi.org/10.1134/S1021443709010166

Lü, F., Wang, G., & Jin, H. (2011a). Photosynthetic responses of thalli and isolated protoplasts of *Bryopsis hypnoides* (Bryopsidales, Chlorophyta) during dehydration. *Chinese Journal of Oceanology and Limnology*, *29*(2), 334–342. https://doi.org/10.1007/s00343-011-0028-4

Lü, F., Xü, W., Tian, C., Wang, G., Niu, J., Pan, G., & Hu, S. (2011b). The *Bryopsis hypnoides* plastid genome: Multimeric forms and complete nucleotide sequence. *PLoS ONE*, *6*(2). https://doi.org/10.1371/journal.pone.0014663

Mahmood, T., & Yang, P. C. (2012). Western blot: Technique, theory, and trouble shooting. *North American Journal of Medical Sciences*, *4*(9), 429–434. https://doi.org/10.4103/1947-2714.100998

Mattoo, A. K., Hoffman-Falk, H., Marder, J. B., & Edelman, M. (1984). Regulation of protein metabolism: coupling of photosynthetic electron transport to in vivo degradation of the rapidly metabolized 32-kilodalton protein of the chloroplast membranes. *Isotopenpraxis*, *20*(1), 1380–1384. https://doi.org/10.1073/pnas.81.5.1380

Müller, P., Li, X. P., & Niyogi, K. K. (2001). Non-photochemical quenching. A response to excess light energy. *Plant Physiology*, *125*(4), 1558–1566. https://doi.org/10.1104/pp.125.4.1558

Nishiyama, Y., & Murata, N. (2014). Revised scheme for the mechanism of photoinhibition and its application to enhance the abiotic stress tolerance of the photosynthetic machinery. *Applied Microbiology and Biotechnology*, *98*(21), 8777–8796. https://doi.org/10.1007/s00253-014-6020-0

Nishiyama, Y., Yamamoto, H., Allakhverdiev, S. I., Inaba, M., Yokota, A., & Murata, N. (2001). Oxidative stress inhibits the repair of photodamage to the photosynthetic machinery. *EMBO Journal*, *20*(20), 5587–5594. https://doi.org/10.1093/emboj/20.20.5587

Ohnishi, N., & Murata, N. (2006). Glycinebetaine counteracts the inhibitory effects of salt stress on the degradation and synthesis of D1 protein during photoinhibition in *Synechococcus sp. PCC 7942. Plant Physiology*, *141*(2), 758–765. https://doi.org/10.1104/pp.106.076976

Rantala, S., Järvi, S., & Aro, E.-M. (2021). Photosynthesis | Photosystem II: assembly and turnover of the reaction center D1 Protein in plant chloroplasts. *Encyclopedia of Biological Chemistry III*, *April*, 207–214. https://doi.org/10.1016/b978-0-12-809633-8.21404-0

Schägger, H. (2006). Tricine-SDS-PAGE. *Nature Protocols*, *1*(1), 16–22. https://doi.org/10.1038/nprot.2006.4

Serôdio, J., & Lavaud, J. (2011). A model for describing the light response of the nonphotochemical quenching of chlorophyll fluorescence. *Photosynthesis Research*, *108*(1), 61–76. https://doi.org/10.1007/s11120-011-9654-0

Serôdio, J., Schmidt, W., & Frankenbach, S. (2017). A chlorophyll fluorescence-based method for the integrated characterization of the photophysiological response to light stress. *Journal of Experimental Botany*, *68*(5), 1123–1135. https://doi.org/10.1093/jxb/erw492

Serôdio, J., Schmidt, W., Frommlet, J. C., Christa, G., & Nitschke, M. R. (2018). An LED-based multi-actinic illumination system for the high throughput study of photosynthetic light responses. *PeerJ*, *2018*(9), e5589. https://doi.org/10.7717/peerj.5589

Takahashi, S., & Murata, N. (2006). Glycerate-3-phosphate, produced by CO2 fixation in the calvin cycle, is critical for the synthesis of the D1 protein of photosystem II. *Biochimica et Biophysica Acta - Bioenergetics*, *1757*(3), 198–205. https://doi.org/10.1016/j.bbabio.2006.02.002

Tokutsu, R., Fujimura-Kamada, K., Matsuo, T., Yamasaki, T., & Minagawa, J. (2019). The constants flowering complex controls the protective response of photosynthesis in the green alga *Chlamydomonas*. *Nature Communications*, *10*(1), 2–5. https://doi.org/10.1038/s41467-019-11989-x

Towbin, H., Staehelin, T., & Gordon, J. (1979). Electrophoretic transfer of proteins from polyacrylamide gels to nitrocellulose sheets: Procedure and some applications. *Proceedings of the National Academy of Sciences of the United States of America*, *76*(9). https://doi.org/10.1073/pnas.76.9.4350

Tsonev, T. D., & Hikosaka, K. (2003). Contribution of photosynthetic electron transport, heat dissipation, and recovery of photoinactivated photosystem II to photoprotection at different temperatures in *Chenopodium album* leaves. *Plant and Cell Physiology*, *44*(8), 828–835. https://doi.org/10.1093/pcp/pcg107

Tyystjärvi, E. (2013). Photoinhibition of photosystem II*. In *International Review of Cell and Molecular Biology* (Vol. 300). https://doi.org/10.1016/B978-0-12-405210-9.00007-2

Tyystjärvi, E., Ali-Yrkkö, K., Kettunen, R., & Aro, E. M. (1992). Slow degradation of the D1 protein is related to the susceptibility of low-light-grown pumpkin plants to photoinhibition. *Plant Physiology*, *100*(3), 1310–1317. https://doi.org/10.1104/pp.100.3.1310

Tyystjärvi, E., & Aro, E.-M. (1996). The rate constant of photoinhibition, measured in lincomycin-treated leaves, is directly proportional to light intensity. *Proceedings of the National Academy of Sciences of the United States of America*, *93*(5), 2213–2218. https://doi.org/10.1073/pnas.93.5.2213

Verbruggen, H., Ashworth, M., LoDuca, S. T., Vlaeminck, C., Cocquyt, E., Sauvage, T., Zechman, F. W., Littler, D. S., Littler, M. M., Leliaert, F., & De Clerck, O. (2009). A multi-locus time-calibrated phylogeny of the siphonous green algae. *Molecular Phylogenetics and Evolution*, *50*(3), 642–653. https://doi.org/10.1016/j.ympev.2008.12.018

Wang, G. C., & Tseng, C. K. (2006). Culturing the segments of *Bryopsis hypnoides* Lamoroux thalli regenerated from protoplast aggregations. *Journal of Integrative Plant Biology*, *48*(2), 190–196. https://doi.org/10.1111/j.1744-7909.2006.00190.x

Ye, N. H., Wang, G. C., Wang, F. Z., & Zeng, C. K. (2005). Formation and growth of *Bryopsis hypnoides* Lamouroux regenerated from its protoplasts. *Journal of Integrative Plant Biology*, *47*(7), 856–862. https://doi.org/10.1111/j.1744-7909.2005.00050.x